

PAPER • OPEN ACCESS

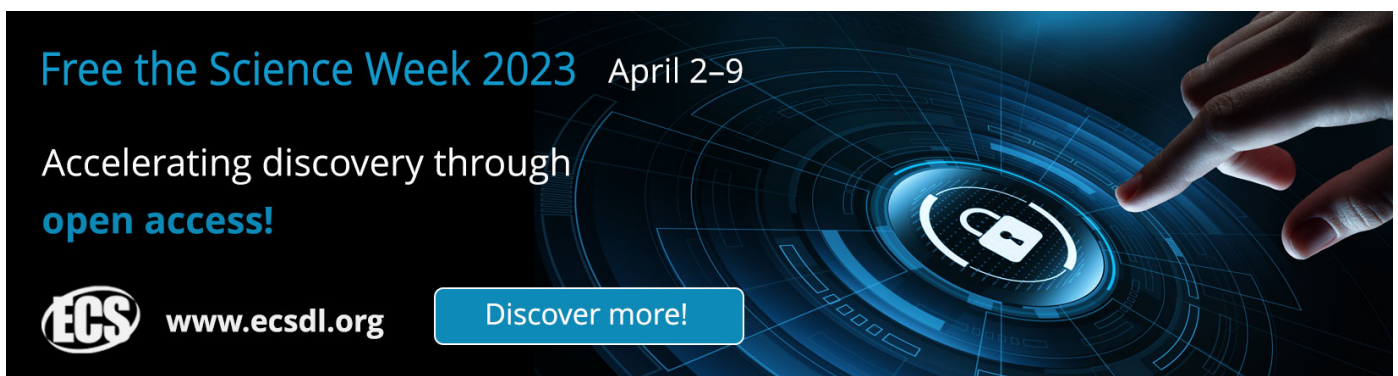
Aspects of isentropic trajectories in chiral effective models

To cite this article: Rainer Stiele *et al* 2020 *J. Phys.: Conf. Ser.* **1667** 012043

View the [article online](#) for updates and enhancements.

You may also like

- [On the expanding configurations of viscous radiation gaseous stars: the isentropic model](#)
Xin Liu
- [A GENERIC formalism for Korteweg-type fluids: I. A comparison with classical theory](#)
Yukihito Suzuki
- [New Models of Jupiter in the Context of Juno and Galileo](#)
Florian Debras and Gilles Chabrier



Free the Science Week 2023 April 2–9

Accelerating discovery through
open access!

 www.ecsdl.org [Discover more!](#)

The banner features a dark blue background with a futuristic, glowing interface. A hand is shown interacting with a circular element containing a padlock icon, symbolizing the removal of access barriers. The text is in white and light blue, with the ECS logo and website URL in white.

Aspects of isentropic trajectories in chiral effective models

Rainer Stiele^{1,2,3}, Wanda Maria Alberico^{1,4}, Andrea Beraudo¹, Renan Câmara Pereira⁵, Pedro Costa⁵, Hubert Hansen³ and Mario Motta^{1,4}

¹ INFN – Sezione di Torino, Via Pietro Giuria 1, I-10125 Torino, Italy

² Univ Lyon, ENS de Lyon, Département de Physique, F-69342, Lyon, France

³ Univ Lyon, Univ Claude Bernard Lyon 1, CNRS/IN2P3, IP2I Lyon, F-69622, Villeurbanne, France

⁴ Dipartimento di Fisica, Università degli Studi di Torino, Via Pietro Giuria 1, I-10125 Torino, Italy

⁵ CFisUC, Department of Physics, University of Coimbra, P-3004 - 516 Coimbra, Portugal

E-mail: r.stiele@ip2i.in2p3.fr

Abstract. The evolution of the fireball in heavy ion collisions is an isentropic process, meaning that it follows a trajectory of constant entropy per baryon in the phase diagram of the strong interaction. The collective acceleration of the system is determined by the speed of sound, while fluctuations of conserved charges are encoded in quark-number susceptibilities: together, they leave their imprint in final observables. Here, this isentropic evolution will be analysed within chiral effective models that account for both chiral and center symmetry breaking, two central aspects of QCD. Our discussion focusses on the impact on the isentropic trajectories of the treatment of high-momentum modes, of the meson contribution to thermodynamics and of the number of quark flavours.

1. Introduction

Chiral effective models allow one to study two important properties of QCD, namely the confinement of constituent quarks with large effective masses at low temperature/density and their deconfinement to light quarks in the hot/dense partonic phase. Generation of constituent quark masses m_f can be described by dynamical breaking of chiral symmetry and deconfinement by spontaneous breaking of center symmetry. The interaction between constituent quarks can be described either as a point-like interaction or by the exchange of a meson. The former leads to what is called the Nambu–Jona-Lasinio (NJL) model [1, 2] and the latter to the Quark-Meson (QM) model [3]. The order parameter of center symmetry breaking, the Polyakov loop Φ can be coupled to these models. This allows to explore phenomenologically with them the phase diagram of strongly-interacting matter [4, 5]. Their Lagrangian can be written as a part describing the spontaneous breaking of chiral symmetry, a kinetic contribution of the quarks that contains a minimal coupling to the gauge field A_μ and the Polyakov-loop potential \mathcal{U}

$$\mathcal{L}_{\text{PNJL/PQM}} = \mathcal{L}_{\text{chiral}} + \bar{q} [i\gamma_\mu (D^\mu + \widehat{\mu}_f \delta^{\mu 0})] q - \mathcal{U}(\Phi[A_\mu], \bar{\Phi}[A_\mu]; T). \quad (1)$$

While the first part differs in the NJL and QM models, the other two contributions are common to both [6, 7]. This structure is conserved for the grand canonical potential in mean-field



Content from this work may be used under the terms of the [Creative Commons Attribution 3.0 licence](https://creativecommons.org/licenses/by/3.0/). Any further distribution of this work must maintain attribution to the author(s) and the title of the work, journal citation and DOI.

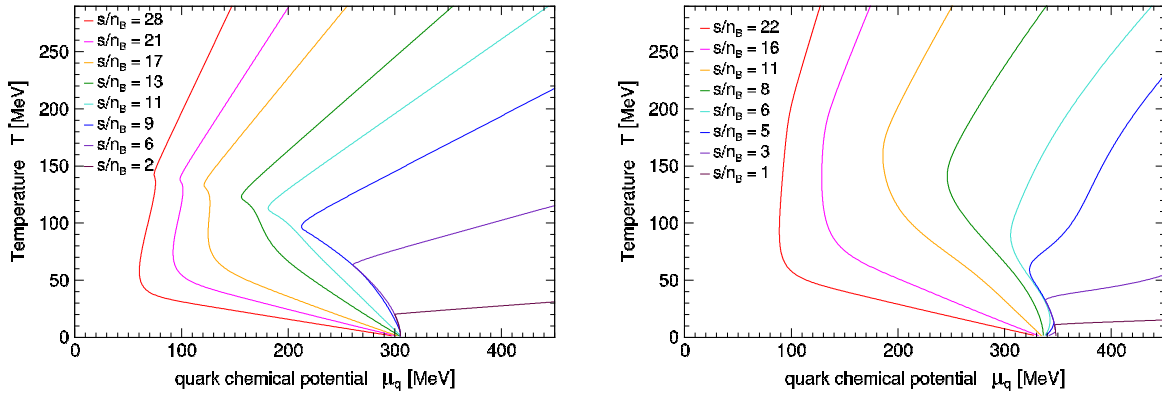


Figure 1. Isentropic lines in the $N_f=2$ Quark-Meson model (left panel) and NJL model (right panel) as in Fig. 9 of Ref. [12].

approximation,

$$\Omega(m_f, \Phi, \bar{\Phi}; T, \mu_f) = U_{\text{chiral}}(m_f) + \Omega_{\bar{q}q}(m_f, \Phi, \bar{\Phi}; T, \mu_f) + \mathcal{U}(\Phi, \bar{\Phi}; T). \quad (2)$$

All thermodynamic quantities can be derived from Eq. (2) ensuring the Gibbs-Duhem relation,

$$p = -\Omega, \quad s = \left. \frac{\partial p}{\partial T} \right|_{\mu_f = \text{const}}, \quad n_f = \left. \frac{\partial p}{\partial \mu_f} \right|_{T = \text{const}} \quad \text{and} \quad \epsilon = Ts - p + \sum_{N_f} \mu_f n_f. \quad (3)$$

Here, several results for the trajectories with constant s/n_q ratio, corresponding to the isentropic evolution of the matter produced in relativistic heavy-ion collisions, will be discussed¹. An in-depth analysis together with the evaluation along these trajectories of thermodynamic quantities like the speed of sound – responsible for the collective acceleration of the fireball – and generalised quark-number susceptibilities – connected to the fluctuations of conserved charges – will be given in Refs. [7, 11].

2. Impact of the UV cutoff

Figure 1 shows isentropic lines in the QM model (left panel) and NJL model (right panel), as presented in Ref. [12] and similarly in Ref. [13]. Isentropic trajectories look quite different in the two models: we wish to analyse such an issue more deeply.

The quark contribution to the grand canonical potential (2) can be written as the sum of two contributions. One is a vacuum-like term that does not depend *explicitly* on medium properties like temperature or chemical potential,

$$\Omega_{\bar{q}q}^{\text{vac}}(m_\ell, m_s) = -2N_c \sum_f \int \frac{d^3k}{(2\pi)^3} E_f \stackrel{\text{QM}}{=} -\frac{N_c}{8\pi^2} \sum_f m_f^4 \ln\left(\frac{m_f}{\Lambda}\right). \quad (4)$$

In the above the integral over the three-momentum is divergent and requires an ultra-violet cutoff Λ . However, the divergence can be renormalised in the QM model [14].² The other

¹ Indeed, for AGS, SPS, and RHIC, the values of s/n_B are, respectively, 30, 45, and 300 [8]. At these values, lattice results for the isentropic (2+1)-flavour equation of state were obtained in Refs. [9, 10].

² The formal dependence of Eq. (4) on the cutoff is cancelled in the renormalised QM model by a formal dependence of the parameters of $U_{\text{chiral}}^{\text{QM}}$ on the cutoff such that Eq. (2) and derived equations are cutoff independent.

Figure 2. Impact of the UV cutoff on the isentropic trajectories in the NJL model. The dashed curves are the ones shown in the right panel of Fig. 1 and are obtained applying the UV cutoff to all momentum integrals. The solid curves are obtained applying the UV cutoff only to the divergent integral over the vacuum fluctuations. In this case, the shape of the lines of constant entropy per quark is closer to those of the Quark-Meson model, shown in the left panel of Fig. 1.

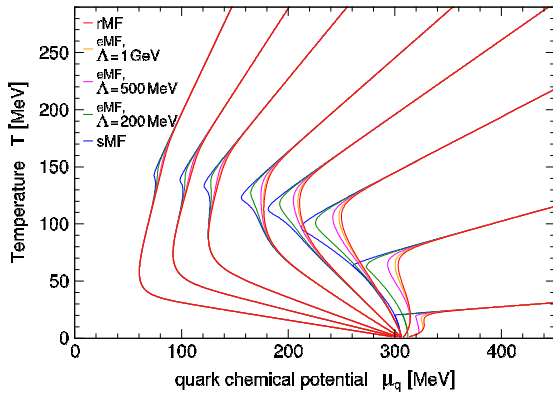
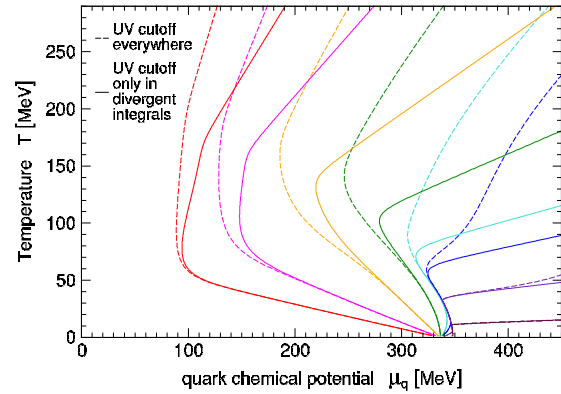


Figure 3. Impact of the cutoff scale in (4) on the isentropic trajectories in a Quark-Meson model calculation. The blue lines are the ones shown in the left panel of Fig. 1. sMF stands for standard mean-field model ($\Lambda = 0$), eMF for extended mean-field model ($\Lambda \in]0, \infty[$) and rMF for renormalised mean-field model ($\hat{=} \Lambda \rightarrow \infty$).

contribution contains the quark and anti-quark distribution functions that are defined e.g. in [6]

$$\Omega_{\text{qq}}^{\text{th}}(m_f, \Phi, \bar{\Phi}; T, \mu_f) = -2T \sum_f \int^{\Lambda, \infty} \frac{d^3k}{(2\pi)^3} [z_f(m_f, \Phi, \bar{\Phi}; T, \mu_f) + z_{\bar{f}}(m_f, \Phi, \bar{\Phi}; T, \mu_f)] . \quad (5)$$

It is therefore a convergent integral and in the QM model there is no reason to apply a UV cutoff. In the NJL model the situation is different. One can either define the whole theory with a UV cutoff and apply the one of (4) also to (5) as is done for the NJL result in Fig. 1. Otherwise, in order not to lose a relevant contribution from high-momentum modes to thermodynamics, one can apply the UV cutoff only to the divergent integral (4). Figure 2 shows the impact of applying the cutoff Λ to the non-divergent integrals: the shape of the lines of constant entropy per particle in the NJL model is closer to the one of the QM model when integrating up to infinity in all convergent thermal integrals. A detailed discussion can be found in Ref. [15].

Furthermore, the cutoff in Eq. (4) should be chosen large enough to have little quantitative impact on the results. The QM model allows one to study how the results converge when increasing the UV cutoff scale from zero (considered as the standard mean-field (sMF) analysis in the QM model, applied in Ref. [12] to obtain the results in the left panel of Fig. 1) towards the renormalised mean-field (rMF) model, see Fig. 3.

3. Impact of contribution of mesons to thermodynamics

In the common mean-field approximation of (P)QM/(P)NJL models only thermal fluctuations of quarks contribute to the thermodynamic potential, while any thermal contribution from the

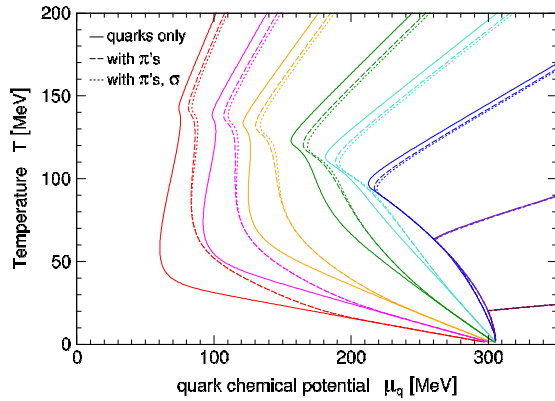


Figure 4. Impact of the contribution of mesons to the isentropic trajectories. The solid lines are those in the left panel of Fig. 1 and with quarks only, the dashed lines are with an additional contribution of a pion gas to thermodynamics and the dotted line with a pion and σ -meson gas contribution.

mesons is neglected.

To achieve a better description of thermodynamics in the phase where mesons are the dominant degrees of freedom, the thermodynamics can be augmented by the contribution of a gas of thermal mesons [16, 17]. The contribution to the pressure of each meson species ϕ_i is

$$p_{\phi_i} = \frac{1}{(2\pi)^3} \int_0^\infty d^3k \frac{k^2}{3E_{\phi_i}} \frac{1}{e^{(E_{\phi_i} - \mu_{\phi_i})/T} - 1} \quad \text{with} \quad E_{\phi_i} = \sqrt{k^2 + m_{\phi_i}^2}. \quad (6)$$

The total contribution of the mesons to the pressure p_ϕ is accordingly $p_\phi = \sum_i p_{\phi_i}$ and overall $p = -\Omega + p_\phi$. The meson masses that enter into the dispersion relations of the mesons in Eq. (6) are medium dependent. This medium dependence of the meson masses makes the pressure of the mesons p_ϕ strictly speaking a field(ψ_i)-dependent correction to the thermodynamical potential that contributes as well to the equations of motion, $\partial\Omega/\partial\psi_i - \partial p_\phi/\partial\psi_i$ and the meson masses themselves. In a lowest order approximation this correction could be neglected, assuming that the dynamics of the system is governed by the grand canonical potential Ω alone which determines the meson masses as well. An uncoupled meson gas with these meson masses is then added to thermodynamics via $p = -\Omega + p_\phi$. All thermodynamic quantities are derived from this equation ensuring the Gibbs-Duhem relation. All contributions stemming from $\partial p_\phi/\partial\psi_i$ are neglected there consistently as well.

The considerable impact on the isentropic trajectories when including the meson contribution to thermodynamics is shown in Fig. 4 in a QM model calculation, see also Refs. [18, 19] for calculations using the Functional Renormalization Group.

4. Impact of the number of quark flavours

Isentropic lines in the PNJL model when strangeness is included were obtained in [20, 21, 22] for different scenarios. Interestingly enough, the impact of including the strange quark in the calculation on the isentropic trajectories shown in Fig. 5 for the QM model is quite mild, less relevant than including the contribution of light mesons to thermodynamics, as shown in Fig. 4.

5. Outlook

A complete discussion of isentropic trajectories and of their potential to experimentally identify the presence of a critical end-point thanks to quantities like the speed of sound – responsible for the collective acceleration of the fireball – and quark-number susceptibilities – connected to the fluctuations of conserved charges – will be given in Ref. [11]. They will be also addressed within a systematic comparison between the (P)NJL and (P)QM frameworks in Ref. [7] and the impact

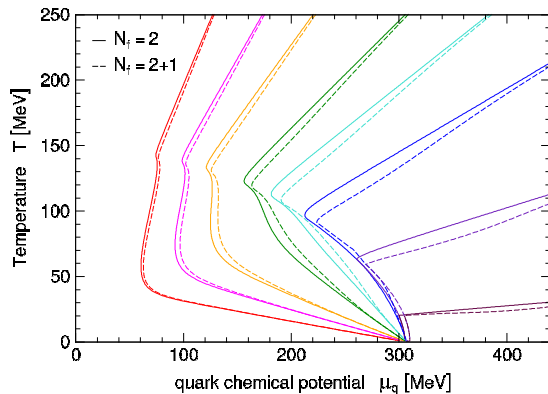


Figure 5. Impact of the number of quark flavours on the isentropic lines. The solid lines are those in the left panel of Fig. 1 and the dashed ones the corresponding ones in a $N_f = 2+1$ –flavour calculation.

of an improvement of the Polyakov-loop potential [23] will be analysed. The importance of lines of constant entropy to analyse the low-temperature/high-density phase within the Functional Renormalization Group approach will be discussed in Ref. [24]. A discussion on finite size effects on isentropic trajectories can be found in Ref. [25].

Acknowledgments

This work was supported by an INFN Post Doctoral Fellowship (competition INFN notice n. 18372/2016, RS) as well as by STSM Grants from the COST Action CA15213 “Theory of hot matter and relativistic heavy-ion collisions” (THOR) (RCP, PC, HH, MM, RS) and we thank for support and hospitality of CFisUC (project UID/FIS/04564/2016 - FCT Portugal).

References

- [1] Nambu Y and Jona-Lasinio G 1961 *Phys. Rev.* **122** 345–358
- [2] Nambu Y and Jona-Lasinio G 1961 *Phys. Rev.* **124** 246–254
- [3] Gell-Mann M and Levy M 1960 *Nuovo Cim.* **16** 705
- [4] Mocsy A, Sannino F and Tuominen K 2004 *Phys. Rev. Lett.* **92** 182302 (*Preprint hep-ph/0308135*)
- [5] Fukushima K 2004 *Phys. Lett. B* **591** 277–284 (*Preprint hep-ph/0310121*)
- [6] Hansen H, Stiele R and Costa P 2019 (*Preprint 1904.08965*)
- [7] Câmara Pereira R, Costa P, Hansen H, Motta M and Stiele R 2019 In preparation
- [8] Bluhm M, Kampfer B, Schulze R, Seipt D and Heinz U 2007 *Phys. Rev. C* **76** 034901 (*Preprint 0705.0397*)
- [9] DeTar C, Levkova L, Gottlieb S, Heller U M, Hetrick J E, Sugar R and Toussaint D 2010 *Phys. Rev. D* **81** 114504 (*Preprint 1003.5682*)
- [10] Borsanyi S, Endrodi G, Fodor Z, Katz S, Krieg S *et al.* 2012 *JHEP* **1208** 053 (*Preprint 1204.6710*)
- [11] Motta M, Stiele R, Alberico W M and Beraudo A 2019 In preparation
- [12] Scavenius O, Mocsy A, Mishustin I and Rischke D 2001 *Phys. Rev. C* **64** 045202 (*Preprint nucl-th/0007030*)
- [13] Kahara T and Tuominen K 2008 *Phys. Rev. D* **78** 034015 (*Preprint 0803.2598*)
- [14] Skokov V, Friman B, Nakano E, Redlich K and Schaefer B J 2010 *Phys. Rev. D* **82** 034029 (*Preprint 1005.3166*)
- [15] Costa P, Hansen H, Ruivo M C and de Sousa C A 2010 *Phys. Rev. D* **81** 016007 (*Preprint 0909.5124*)
- [16] Haas L M, Stiele R, Braun J, Pawlowski J M and Schaffner-Bielich J 2013 *Phys. Rev. D* **87**(7) 076004 (*Preprint 1302.1993*)
- [17] Herbst T K, Mitter M, Pawlowski J M, Schaefer B J and Stiele R 2014 *Phys. Lett. B* **731** 248–256 (*Preprint 1308.3621*)
- [18] Nakano E, Schaefer B J, Stokic B, Friman B and Redlich K 2010 *Phys. Lett. B* **682** 401–407 (*Preprint 0907.1344*)
- [19] Skokov V, Friman B and Redlich K 2011 *Phys. Rev. C* **83** 054904 (*Preprint 1008.4570*)
- [20] Fukushima K 2009 *Phys. Rev. D* **79** 074015 (*Preprint 0901.0783*)
- [21] Costa P, Ruivo M, de Sousa C and Hansen H 2010 *Symmetry* **2** 1338–1374 (*Preprint 1007.1380*)
- [22] Costa P 2016 *Phys. Rev. D* **93** 114035 (*Preprint 1610.06433*)
- [23] Baillot N, Hansen H and Stiele R 2019 In preparation
- [24] Câmara Pereira R and Stiele R 2019 In preparation
- [25] Palhares L F, Fraga E S and Kodama T 2011 *J. Phys. G* **38** 085101 (*Preprint 0904.4830*)